

Very low 1/f barrier noise in sputtered MgO magnetic tunnel junctions with high tunneling magnetoresistance

J. F. Feng, J. Y. Chen, H. Kurt, and J. M. D. Coey

Citation: [Journal of Applied Physics](#) **112**, 123907 (2012); doi: 10.1063/1.4769805

View online: <http://dx.doi.org/10.1063/1.4769805>

View Table of Contents: <http://scitation.aip.org/content/aip/journal/jap/112/12?ver=pdfcov>

Published by the [AIP Publishing](#)

Articles you may be interested in

[Influence of growth and annealing conditions on low-frequency magnetic 1/f noise in MgO magnetic tunnel junctions](#)

J. Appl. Phys. **112**, 093913 (2012); 10.1063/1.4764314

[1 / f noise in MgO double-barrier magnetic tunnel junctions](#)

Appl. Phys. Lett. **98**, 112504 (2011); 10.1063/1.3562951

[Boron diffusion in magnetic tunnel junctions with MgO \(001\) barriers and CoFeB electrodes](#)

Appl. Phys. Lett. **96**, 262501 (2010); 10.1063/1.3457475

[Strongly suppressed 1/f noise and enhanced magnetoresistance in epitaxial Fe-V/MgO/Fe magnetic tunnel junctions](#)

Appl. Phys. Lett. **96**, 202501 (2010); 10.1063/1.3430064

[1 f noise in magnetic tunnel junctions with MgO tunnel barriers](#)

J. Appl. Phys. **99**, 08A906 (2006); 10.1063/1.2169591

High-Voltage Amplifiers

- Voltage Range from $\pm 50V$ to $\pm 60kV$
- Current to 25A

Electrostatic Voltmeters

- Contacting & Non-contacting
- Sensitive to 1mV
- Measure to 20kV



ENABLING RESEARCH AND
INNOVATION IN DIELECTRICS,
ELECTROSTATICS,
MATERIALS, PLASMAS AND PIEZOS



www.trekinc.com

TREK, INC. 190 Walnut Street, Lockport, NY 14094 USA • Toll Free in USA 1-800-FOR-TREK • (t):716-438-7555 • (f):716-201-1804 • sales@trekinc.com

Very low $1/f$ barrier noise in sputtered MgO magnetic tunnel junctions with high tunneling magnetoresistance

J. F. Feng, J. Y. Chen, H. Kurt, and J. M. D. Coey
 CRANN and School of Physics, Trinity College, Dublin 2, Ireland

(Received 24 October 2012; accepted 17 November 2012; published online 19 December 2012)

Low frequency $1/f$ barrier noise has been investigated in sputtered MgO magnetic tunnel junctions (MTJs) with a tunneling magnetoresistance ratio of up to 330% at room temperature. The lowest normalized noise parameter α of the tunnel barrier reaches 2.5×10^{-12} – $2.1 \times 10^{-11} \mu\text{m}^2$, which is comparable to that found in MTJs with the MgO barrier grown by MBE or electron-beam evaporation. This normalized barrier noise is almost bias independent in the voltage range of up to ± 1.2 V. The low noise level and high voltage stability may reflect the high quality of the sputtered MgO with a uniform distribution of defects in the MgO layer. © 2012 American Institute of Physics. [<http://dx.doi.org/10.1063/1.4769805>]

I. INTRODUCTION

Since the beginning of this century, magnetic tunnel junctions (MTJs) with crystalline MgO barriers have become an active area of research,^{1–4} following predictions by theory of a large magnetoresistance with bcc Fe or CoFe electrodes.^{5,6} This is due to interesting fundamental physics as well as significant technological potential applications for these MTJ devices.⁷ The latter have been usually demonstrated in sputtered and annealed CoFeB/MgO junctions.^{3,4} Besides the requirement of high tunneling magnetoresistance (TMR) for MTJ devices, the low frequency noise level is of significance for practical applications.

The low frequency noise in MTJs is often associated with the $1/f$ noise in parallel (P) and antiparallel (AP) states.^{8,9} The $1/f$ noise in the P state mainly reflects the spin-independent resistance fluctuations in the tunneling barrier,¹⁰ which are usually due to localized charge traps.^{10–12} The barrier noise sets the minimum noise level in any type of MTJ device. $1/f$ noise can be characterized by a parameter $\alpha = AfS_V/V^2$ (units in μm^2), where A is the junction area, f is the frequency, S_V is the noise power spectral density, and V is the applied voltage.¹² Until now, the barrier noise level for sputtered MgO MTJs has been reported to be 1 – $3 \times 10^{-10} \mu\text{m}^2$ at room temperature.^{10,13–15} Improving the quality of the MgO can result in a lower barrier noise level in MTJs due to a lower density of defects and less disorder. The best barrier noise has been achieved in MTJs with MgO barriers grown by MBE¹⁶ or electron-beam evaporation,¹¹ where it reaches 1 – $3 \times 10^{-11} \mu\text{m}^2$ at 300 K. Moreover, at 4 K, a barrier noise level as low as 2.7 – $9.6 \times 10^{-13} \mu\text{m}^2$ in sputtered CoFeB/MgO/CoFeB MTJs¹⁰ and 1 – $1.3 \times 10^{-12} \mu\text{m}^2$ in epitaxial Fe/MgAl₂O_x/Fe MTJs¹⁷ has been reported. However, the barrier noise of MTJs at low temperature is around two orders of magnitude lower than that at 300 K.¹⁰

Here, we report a low barrier noise and high TMR at room temperature for sputtered MgO MTJs with resistance-area (RA) values of order $10^4 \Omega \mu\text{m}^2$. The noise in the P state (α_P) at 300 K is comparable to that in MTJs with MgO grown by MBE¹⁶ or electron-beam evaporation.¹¹ Furthermore, a

room-temperature TMR up to 330% has been achieved in these exchange-biased MTJ devices with 0.9 nm Ru in CoFe/Ru/CoFeB synthetic antiferromagnetic (SAF) pinned layers, which is a little higher than reported previously in similar stacks with the same Ru thickness.¹⁸ The α_P values have also been investigated as function of the bias voltage and junction area, and a very weak dependence of α_P has been found for both cases.

II. EXPERIMENTS

The MTJ stacks were deposited at room temperature on thermally oxidized Si substrates, with the layer sequence Ta 5/Ru 30/Ta 5/Ni₈₁Fe₁₉ 5/Ir₂₂Mn₇₈ 10/Co₉₀Fe₁₀ 2.5/Ru 0.9/Co₄₀Fe₄₀B₂₀(CoFeB) 3/MgO $t = 1.8$ or 2.0/CoFeB 3/Ta 5/Ru 5 (thickness in nm). After deposition of the bottom electrodes by dc sputtering in the HV chamber with a base pressure of 1×10^{-7} Torr in our Sharmrock cluster deposition system, the MgO layers were grown by RF sputtering from two MgO targets in a target-facing-target gun, in another chamber of the same system having a base pressure less than 1×10^{-8} Torr. Then top electrodes were sputtered. All MTJ layers were deposited without breaking the vacuum during the growth process. The growth pressure for the MgO layer was varied from 1.3 to 4.0 mTorr. Here, we select two series of MTJs for noise and TMR study, A-series MTJs are these with $t = 1.8$ nm grown at 1.3 mTorr, and B-series MTJs have $t = 2.0$ nm grown at 4 mTorr. The MTJs were fabricated by UV lithography and Ar ion milling with junction area ranging from 10 to 1000 μm^2 . High vacuum post-annealing was performed in the temperature range of 325–425 °C in an applied magnetic field of 800 mT for 0.5 h. Both the TMR ratio and noise become stable when the annealing time is several tens of minutes (e.g., 15 min).¹³ All measurements were made at room temperature.

III. RESULTS AND DISCUSSION

Figure 1 presents the TMR versus magnetic field curve of a MTJ with $t = 1.8$ nm annealed at 400 °C, having the RA products of $2.4 \times 10^4 \Omega \mu\text{m}^2$ in the P state. A TMR of 274%

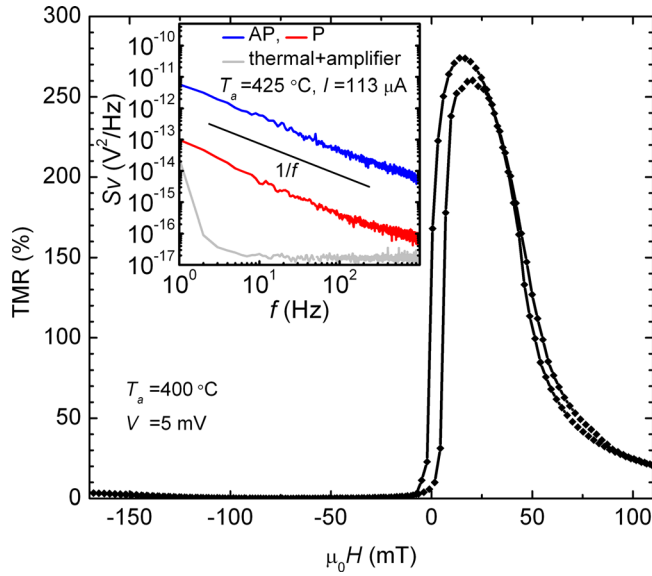


FIG. 1. TMR versus magnetic field for an MTJ with a 1.8 nm MgO barrier. The inset shows the noise power spectral density (S_V) as a function of frequency in the P and AP states, as well as the thermal noise and the amplifier noise. The line in the inset is a guide to the eye for $1/f$ noise.

is observed at room temperature. The inset of Fig. 1 shows the noise power spectrum density (S_V) as a function of frequency. A $1/f$ spectrum is observed in both P and AP states, where thermal noise and amplifier noise have been subtracted. Here, we apply magnetic fields of 80 and -20 mT to measure the noise in both resistance states for these sputtered MgO MTJs. It is found that S_V in the P state is independent of magnetic field; it is essentially just the barrier noise.

In Figure 2, the annealing temperature (T_a) dependence of TMR and α_P at a low bias is plotted for A- and B-MTJs with small junction area. As T_a increases from 325 °C, the TMR values increase, which suggests an improved quality of the MgO layer and the CoFeB/MgO interfaces. As reported in Ref. 19, elimination of point defects and quality improve-

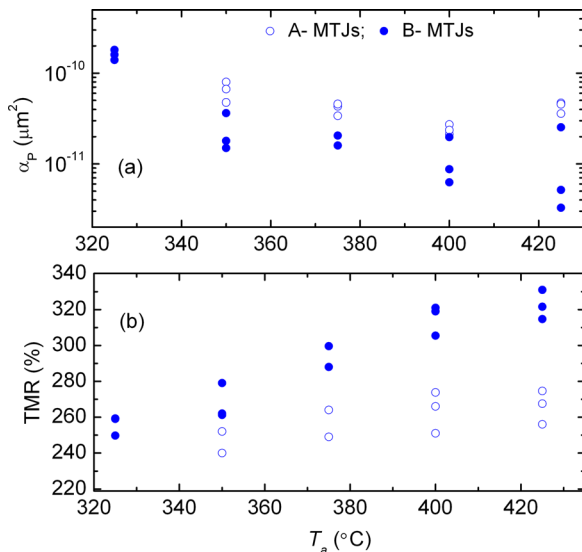


FIG. 2. The annealing temperature (T_a) dependence of α_P (a) and TMR (b) for both A-MTJs (1.8 nm MgO) and B-MTJs (2.0 nm MgO).

ment in MgO due to the annealing treatment results in the magnetoresistance improvement. Higher TMR can be obtained for MTJs with thicker MgO barrier, which may result in a little difference of TMR for A- and B-MTJs. Furthermore, the MgO quality may influence TMR (see the discussion below). α_P is also found to depend on T_a ; lower α_P can be achieved at higher T_a , which is supported by a recent report on similar MTJs.¹³ At $T_a = 400$ °C, both TMR and α_P approach saturation at their maximum and minimum values, respectively. The lowest α_P value for A-MTJs is $2.1 \times 10^{-11} \mu\text{m}^2$ at $T_a = 400$ °C, which is almost one order of magnitude lower than previously reported in sputtered MgO MTJs.^{13–15} Furthermore, the lowest α_P value for B-MTJs is even lower compared with A-MTJs, reaching $2.5\text{--}3.3 \times 10^{-12} \mu\text{m}^2$ at $T_a = 400$ °C, which only appears under a large magnetic field of either polarity. The highest TMR for B-MTJs reaches 330% at $T_a = 425$ °C. Both the high TMR and low barrier noise may reflect the quality of the MgO barriers and the CoFeB/MgO interfaces in our sputtered MTJs.

To demonstrate the quality of our sputtered MgO layer, TMR and α in the P and AP states for A-MTJs are plotted as a function of the junction area (A) in the range of $10\text{--}1000 \mu\text{m}^2$. These data are taken at $T_a = 425$ °C, as shown in Fig. 3. The TMR values are in the range of 254%–273%. Here, α , especially in the P state, is quite stable with increasing junction area; it increases by a factor of two with 100 times increase of junction area, reflecting the nearly-perfect quality of the MgO barrier (see the discussion below). The MgO grain size is uniform; accordingly, the vacancy defects in the MgO layer and at the CoFeB/MgO interfaces also have a uniform distribution. No pinholes exist in our sputtered MgO. All of these factors may be responsible for the weak area dependence of α in both P and AP states shown in Fig. 3.

As presented in Figure 4, 2θ x-ray diffraction (XRD) scans show 22 nm MgO annealed at high temperature is almost bulk-like ($2\theta = 42.75^\circ$ in our MgO compared with 42.9° for the bulk case). Moreover, the full width at half maximum of the 002 peak, which gives an idea of the crystal

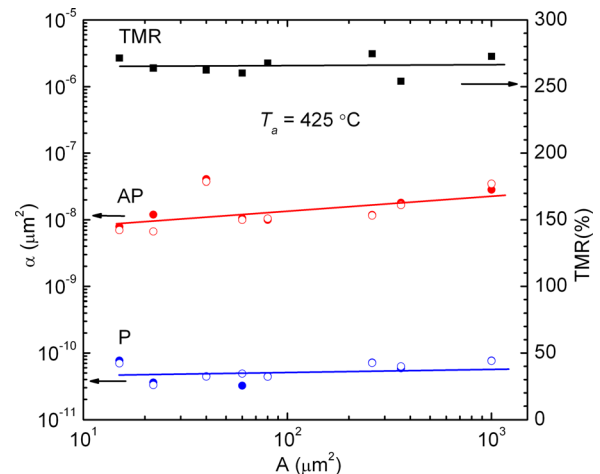


FIG. 3. TMR and α in the P and AP states as a function of the junction area (A) for A-MTJs at $T_a = 425$ °C. Their RA products are $2\text{--}3 \times 10^4 \mu\text{m}^2$ in the P state.

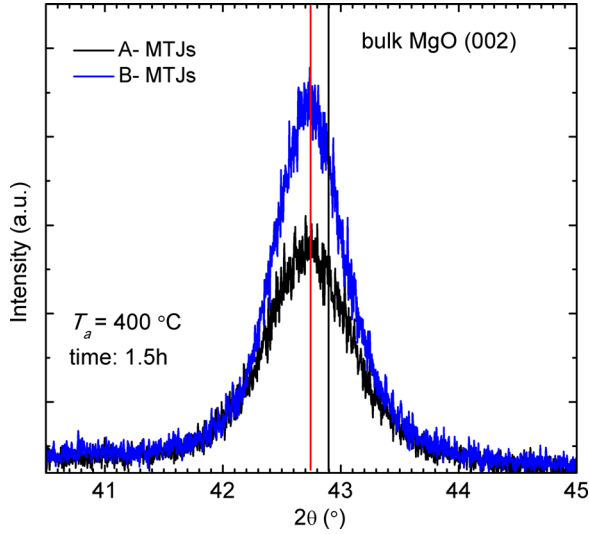


FIG. 4. 2θ XRD scans of 22 nm MgO grown at 1.3 mTorr and 4.0 mTorr like those used in A- and B-MTJ structures, annealed at 400 °C for 1.5 h which is sufficient to form a good MgO/CoFeB interfaces. The black line shows the 2θ position of bulk MgO (002). The red line is a guide to the eye.

quality, is higher for samples grown at 1.3 mTorr. This indicates that the MgO quality is a little poorer for samples with a low growth pressure. Because higher pressure leads to bigger grain size due to a fast growth rate, the averaged grain sizes for 1.3 mTorr and 4.0 mTorr are 10.7 and 12.8 nm when the thickness of MgO is 22 nm. Although the grain size reduces to several nanometers when the MgO layer is thin,²⁰ it may remain a little bigger for B-MTJ samples. Moreover, according to the results in Ref. 21, the interface quality is similar for A- and B-MTJs when the growth pressure of MgO is in the range of 1.3–4.0 mTorr. The improvement of TMR and noise for B-MTJs shown in Fig. 2 may be related to the increase of barrier quality and the decrease in grain boundary density (lower density of defects) of the MgO layer where coherent tunneling of Δ_1 electrons is not restricted.²²

Figure 5 shows the bias dependence of the normalized differential resistance dV/dI and α in the P and AP states for a 1.8 nm MTJ at $T_a = 425$ °C. The bias dependence of both parameters is almost symmetric in these MTJs, which

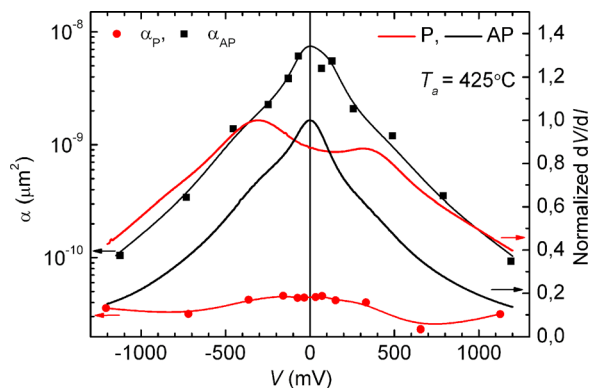


FIG. 5. The bias dependence of α and normalized dV/dI in the P and AP states for A-MTJs at $T_a = 425$ °C. The lines for α in two resistance states are guides to the eye.

reflects the similarity of top and bottom CoFeB/MgO interfaces. In the bias range of up to ± 1.2 V, α_P is almost bias independent. A similar behavior within ± 0.6 V has been observed in MTJs with MgO grown by MBE¹⁶ or electron-beam evaporation.¹¹ Besides, the weak bias dependence of α_P has also been seen within ± 0.5 V in MTJs with sputtered MgO.^{13,15} The voltage dependence of the differential resistance dV/dI is also given in Fig. 5, which is normalized to facilitate the comparison. A bias anomaly of resistance especially in the P state around 0.4 V may be due to the appearance of interfacial states due to defects.²³ After comparing noise and resistance changing with bias, one finds that interfacial states influence both noise and resistance similarly. In the AP state, the nonlinear behavior of α is quite similar to that of dV/dI , in agreement with the results in Refs. 13, 15, and 16. In the P state, α_P follows a similar change with bias up to around 0.7 V compared with dV/dI ,¹⁵ but some deviation occurs at high voltage. Possible shot noise may appear at high voltage.^{24,25} The gradual increase of α_P with bias above 0.7 V may be due to the increase of the shot noise.²⁵ In our case, as shown in Fig. 5, the increase of noise at high voltage due to the shot noise does not alter the barrier noise much.

IV. CONCLUSION

In conclusion, we have measured TMR and low frequency barrier noise in MTJs with sputtered MgO, changing the growth pressure. A TMR of up to 330% and a barrier noise as low as $2.5\text{--}3.3 \times 10^{-12} \mu\text{m}^2$ have been observed at room temperature. The recorded noise parameter in the P state at 300 K is comparable with that in MTJs grown by MBE or electron-beam evaporation. We attribute the behavior to a MgO structure with uniform grains. Accordingly, defects with a uniform distribution and low density may form in the MgO layer. The noise parameter in the P state is almost independent of bias for the range of up to ± 1.2 V. Combined high TMR with low barrier noise may make sputtered MgO MTJ devices more desirable for applications.

ACKNOWLEDGMENTS

JFF thanks Z. Diao for useful discussions. This work was supported by SFI as part of the MANSE Project No. 2005/IN/1850 and was conducted under the framework of the INSPIRE program, funded by the Irish Government's Program for Research in Third Level Institutions, Cycle 4, National Development Plan 2007–2013.

¹S. Yuasa, A. Fukushima, T. Nagahama, K. Ando, and Y. Suzuki, *Nature Mater.* **3**, 868 (2004).

²S. S. Parkin, C. Kaiser, A. Panchula, P. M. Rice, B. Hughes, M. Samant, and S. H. Yang, *Nature Mater.* **3**, 862 (2004).

³D. D. Djayapawira, K. Tsunekawa, M. Nagai, H. Maehara, S. Yamagata, N. Watanabe, S. Yuasa, Y. Suzuki, and K. Ando, *Appl. Phys. Lett.* **86**, 092502 (2005).

⁴S. Ikeda, J. Hayakawa, Y. Ashizawa, Y. M. Lee, K. Miura, H. Hasegawa, M. Tsunoda, F. Matsukura, and H. Ohno, *Appl. Phys. Lett.* **93**, 082508 (2008).

⁵W. H. Butler, X.-G. Zhang, T. C. Schulthess, and J. M. MacLaren, *Phys. Rev. B* **63**, 054416 (2001).

⁶J. Mathon and A. Umersky, *Phys. Rev. B* **63**, 220403 (2001).

- ⁷S. Yuasa and D. D. Djayaprawira, *J. Phys. D* **40**, R337 (2007).
- ⁸J. M. Almeida, R. Ferreira, P. P. Freitas, J. Langer, B. Ocker, and W. Maass, *J. Appl. Phys.* **99**, 08B314 (2006).
- ⁹W. F. Egelhoff, Jr., P. W. T. Pong, J. Unguris, R. D. McMichael, E. R. Nowak, A. S. Edelstein, J. E. Burnette, and G. A. Fischer, *Sens. Actuators A* **155**, 217 (2009).
- ¹⁰J. Scola, H. Polovy, C. Fermon, M. Pannetier-Lecoeur, G. Feng, K. Fahy, and J. M. D. Coey, *Appl. Phys. Lett.* **90**, 252501 (2007).
- ¹¹Z. Diao, J. F. Feng, H. Kurt, G. Feng, and J. M. D. Coey, *Appl. Phys. Lett.* **96**, 202506 (2010).
- ¹²E. R. Nowak, M. B. Weissman, and S. S. P. Parkin, *Appl. Phys. Lett.* **74**, 600 (1999).
- ¹³R. Stearrett, W. G. Wang, L. R. Shah, A. Gokce, J. Q. Xiao, and E. R. Nowak, *J. Appl. Phys.* **107**, 064502 (2010).
- ¹⁴G. Q. Yu, Z. Diao, J. F. Feng, H. Kurt, X. F. Han, and J. M. D. Coey, *Appl. Phys. Lett.* **98**, 112504 (2011).
- ¹⁵J. M. Almeida, P. Wisniewski, and P. P. Freitas, *IEEE Trans. Magn.* **44**, 2569 (2008).
- ¹⁶F. G. Aliev, R. Guerrero, D. Herranz, R. Villar, F. Greullet, C. Tiusan, and M. Hehn, *Appl. Phys. Lett.* **91**, 232504 (2007).
- ¹⁷T. Tanaka, T. Arakawa, K. Chida, Y. Nishihara, D. Chiba, K. Kobayashi, T. Ono, H. Sukegawa, S. Kasai, and S. Mitani, *Appl. Phys. Express* **5**, 053003 (2012).
- ¹⁸Y. M. Lee, J. Hayakawa, S. Ikeda, F. Matsukura, and H. Ohno, *Appl. Phys. Lett.* **89**, 042506 (2006).
- ¹⁹C.-J. Zhao, Y. Liu, J.-Y. Zhang, L. Sun, L. Ding, P. Zhang, B.-Y. Wang, X.-Z. Cao, and G.-H. Yu, *Appl. Phys. Lett.* **101**, 072404 (2012).
- ²⁰C. Tiusan, F. Greullet, M. Hehn, F. Montaigne, S. Andrieu, and A. Schuhl, *J. Phys. Condens. Matter* **19**, 165201 (2007).
- ²¹W. Shen, D. Mazumdar, X. Zou, X. Liu, B. D. Schrag, and G. Xiao, *Appl. Phys. Lett.* **88**, 182508 (2006).
- ²²S. Isogami, M. Tsunoda, K. Komagaki, K. Sunaga, Y. Uehara, M. Sato, T. Miyajima, and M. Takahashi, *Appl. Phys. Lett.* **93**, 192109 (2008).
- ²³F. Bonell, T. Hauet, S. Andrieu, F. Bertran, P. Le Fèvre, L. Calmels, A. Tejada, F. Montaigne, B. Warot-Fonrose, B. Belhadji, A. Nicolaou, and A. Taleb-Ibrahimi, *Phys. Rev. Lett.* **108**, 176602 (2012).
- ²⁴J. P. Cascales, D. Herranz, F. G. Aliev, T. Szczepański, V. K. Dugaev, J. Barnaś, A. Duluard, M. Hehn, and C. Tiusan, *Phys. Rev. Lett.* **109**, 066601 (2012).
- ²⁵K. Liu, K. Xia, and G. E. W. Bauer, *Phys. Rev. B* **86**, 020408(R) (2012).